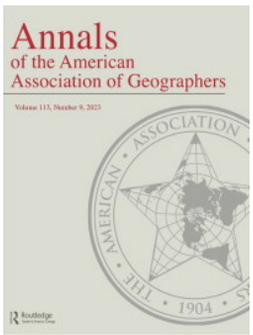

Annals of the American Association of Geographers

ISSN: (Print) (Online) Journal homepage: www.tandfonline.com/journals/raag21

Accumulated Cyclone Energy-Based Tropical Cyclone Return Periods in Florida

Yi-Jie Zhu, Jennifer Collins, Joanne Muller & Philip Klotzbach

To cite this article: Yi-Jie Zhu, Jennifer Collins, Joanne Muller & Philip Klotzbach (2023) Accumulated Cyclone Energy-Based Tropical Cyclone Return Periods in Florida, Annals of the American Association of Geographers, 113:9, 2013-2030, DOI: 10.1080/24694452.2023.2230288

To link to this article: https://doi.org/10.1080/24694452.2023.2230288

Accumulated Cyclone Energy-Based Tropical Cyclone Return Periods in Florida

Yi-Jie Zhu,[*] Jennifer Collins,[*] Joanne Muller,[†] and Philip Klotzbach[‡]

[*]*School of Geosciences, University of South Florida, USA*
[†]*Department of Marine and Earth Sciences, Florida Gulf Coast University, USA*
[‡]*Department of Atmospheric Science, Colorado State University, USA*

This article introduces an accumulated cyclone energy (ACE) approach for estimating the return period of tropical cyclone (TC) wind risk in Florida. As opposed to calculating return periods directly from maximum sustained wind speed, the ACE-based approach also describes the duration of the strong winds, giving an additional dimension to the assessment of TC wind risks. Because Florida is a peninsula, TCs can move across the state within six hours of landfall, causing an underestimation of the inland wind footprint if only the six-hour reanalysis track points are employed as an input data source. This study uses four different scenarios and an inland exponential decay function to interpolate the wind speed between the six-hour reanalysis track points to feed the ACE-based return period calculation based on a 121-year record from 1900 to 2020. South Florida has the shortest return period (five to ten years) of TCs with an ACE equivalent to one hour of hurricane intensity ($\geq$ 64 kt; 1 kt $\sim$ 0.51 m s^{-1}) caused by intense historical hurricane strikes, and Polk County in inland central Florida has an equal return period due to frequent and long-duration TC occurrences, acting as an intersection for landfalling TCs in the Florida peninsula.
Key Words: Florida peninsula, hurricane, inland wind risk.

Among all weather and climate disasters, tropical cyclones (TCs) have dominated both damage and fatalities in the continental U.S. during the past forty years (National Oceanic and Atmospheric Administration [NOAA] 2022). Of all coastal states along the Gulf of Mexico and the Atlantic East Coast, Florida is considered to be the hot spot for TC strikes in terms of frequency and intensity (Blake, Landsea, and Gibney 2011; Jagger and Elsner 2012). The state historically has had about 40 percent of all landfalling hurricanes in the United States based on data from 1851 through 2006 (Blake, Rappaport, and Landsea 2007) and had the second-highest population growth rate nationally, growing by more than 200,000 residents from 1 July 2020 to 1 July 2021 (U.S. Census Bureau 2021). Given the high exposure to TC-related risks, both the emergency management community and the research community have expended considerable effort estimating return periods for TCs in Florida.

Earlier studies have attempted to construct the return period of associated risks from Florida landfalling hurricanes. These include the estimation of the wind risk return period for major cities (Malmstadt, Elsner, and Jagger 2010) and the frequency of TCs that strike the Florida coast (e.g., Keim, Muller, and Stone 2007; Parisi and Lund 2008). Although TCs are expected to diminish rapidly following landfall, recent findings highlighting a weakening of the TC inland decay rate (Li and Chakraborty 2020; Zhu and Collins 2021) and slower inland translation speed (Kossin 2018; Hall and Kossin 2019) have raised the concern for greater and longer exposure of inland communities to TC risks. Moreover, due to the shape of the narrow peninsula, TCs making landfall in Florida tend to maintain most of their intensity while crossing the state (DeMaria, Knaff, and Kaplan 2006; Zhu, Collins, and Klotzbach 2021b). For example, Hurricane Charley in 2004 made landfall at Saffir Simpson Category 4 intensity and remained at hurricane intensity across the state, causing three deaths in two inland counties (Polk and Orange Counties; Federal Emergency Management Agency [FEMA] 2005). Studies that estimate TC return period have mostly focused on the frequency of strikes (not limited to the moment of landfall) and the maximum wind that occurred. The duration of TCs is usually overlooked, however, especially for inland counties that are often less prepared for TC risks. Therefore, we believe that it is

Annals of the American Association of Geographers, 113(9) 2023, pp. 2013–2030
Initial submission, August 2022; revised submissions, November 2022 and February 2023; final acceptance, May 2023
Published by Taylor & Francis, LLC.

important to revisit the return period of TC risk in Florida, particularly accounting for the duration of TC wind over inland areas.

Accumulated cyclone energy (ACE; Bell et al. 2000) has been commonly used as a quantification metric to evaluate seasonal TC activity (Villarini and Vecchi 2012; Collins and Roache 2017; Klotzbach et al. 2018). ACE is defined as the sum of the square of the maximum wind speed for all TCs that are at least of tropical storm ($\geq$34 kt, 1 kt $\approx$ 0.51 m s^{-1}) intensity. Due to its capability of capturing both TC intensity and duration, ACE has also been applied to assess inland TC activity, including seasonal landfall activity (Truchelut and Staehling 2017) and TC postlandfall rate (Zhu, Collins, and Klotzbach 2021a). Therefore, employing ACE as a metric for estimating TC risks has the advantage of including TC wind duration as opposed to just using maximum wind. ACE uses one-minute maximum sustained wind speed (MSW), but it is worth noting that minimum sea-level pressure (MSLP) is also a widely used metric to quantify the intensity of a TC and its damage potential. MSLP has been demonstrated as a more skillful predictor of normalized damage from major hurricanes (Malmstadt, Scheitlin, and Elsner 2009; Klotzbach et al. 2020), due to its improved relationship with storm surge. Apart from other TC risks (e.g., storm surge and rainfall), however, MSW has been shown to be a key indicator of property losses and building damages (Murnane and Elsner 2012; Done, Simmons, and Czajkowski 2018), which is considered more relevant for inland communities.

Using ACE as the primary metric, this study employs a 121-year Florida landfall TC record from 1900 to 2020 to construct TC return period wind risks. A simple algorithm for interpolating inland wind estimates between the six-hour reporting interval of our TC data set (discussed in the next section) is introduced by using a widely applied exponential decay function for inland moving TCs (Kaplan and DeMaria 1995; Li and Chakraborty 2020). The ACE-based return period presented in this article could serve as a reference for implementing TC wind risk mitigation plans, particularly for inland communities. Although the primary analyses in this study are conducted on the ArcGIS platform, the research framework and the logical flow of the study can also be used by researchers from many other geography disciplines as well as the private sector.

Methods

TC Data Set

TC data were taken from the National Hurricane Center's (NHC) North Atlantic hurricane database (HURDAT2; Landsea and Franklin 2013) as archived in the International Best Track Archive for Climate Stewardship (IBTrACS; see https://www.ncdc.noaa.gov/ibtracs/) version 4 (Knapp et al. 2010). Along with several other TC characteristics, the data set reports the location of the storm center (where the MSLP occurs) with a spatial resolution of 0.1° and one-minute averaged MSW at 10 m for each six-hour interval. The MSW reflects the NHC's best estimate of the maximum wind and does not necessarily occur at the storm center but typically occurs within the eyewall. The radius of maximum wind (RMW) has only been tracked since 2004, with an average of 73.7 km (median = 55.6 km) for TCs over Florida. For this study, only TCs that made landfall in the state of Florida with MSW $\geq$ 34 kt are included in this study, yielding a total of 169 landfalling TCs during the period from 1900 to 2020. Data accuracy, including intensity estimates, has increased during the past fifty years with improved satellite coverage and an increased number of coastal weather stations. Although the lack of satellite imagery prior to 1966 could cause underestimates in TCs over the open ocean, landfalling TCs over the continental United States including Florida, are considered relatively reliable since 1900 (Landsea et al. 1999; Landsea 2007; Truchelut, Hart, and Luthman 2013). The accuracy of the wind estimates earlier than the 1960s in the TC data record has improved with the NHC's Atlantic Hurricane Database Reanalysis Project (Delgado, Landsea, and Willoughby 2018).

Inland Wind Estimates

The six-hour interval HURDAT2 best track storm data have been widely used in observational studies on continental U.S. TC landfalls (e.g., Li and Chakraborty 2020; Zhu and Collins 2021; Zhu, Collins, and Klotzbach 2021a). The relatively coarse six-hour interval records, however, are not capable of describing the footprint of inland MSW for fast-moving TCs such as Hurricane Andrew (1992) and Hurricane Charley (2004), both of which crossed the narrow peninsula of Florida within just a few hours of landfall (Pasch, Brown, and Blake 2004). Although previous studies have interpolated inland

wind speed during the six-hour period assuming a linear trend in MSW within the six-hour interval (Kruk et al. 2010) or have used linear or spline interpolation between adjacent track points (Jagger and Elsner 2006; Truchelut and Staehling 2017), the nature of rapid intensity decay from postlandfalling TCs might not be well represented by these methods. Because postlandfall wind decay from TCs generally follows an exponential decay function (Kaplan and DeMaria 1995), the inland MSW estimates at time t (v_t) in between six-hour track points are interpolated in this study as:

$$v_t = v_i \times e^{-a(t-i)} \quad (1)$$

where v_i is the MSW from the preceding six-hour track point at time i ($i < t \leq i+6$), a is the decay constant derived from the adjacent pair of six-hour track points v_i and v_{i+6} :

$$a = [\ln(v_i) - \ln(v_{i+6})]/6 \quad (2)$$

We next divided the six-hour track into 100 parts, with each part equivalent to a temporal resolution of 3.6 minutes. The combination of Equation 1 and Equation 2 was then used to determine the inland wind speed where both v_i and v_{i+6} occurred when the TC was inland (Scenario 1; Figure 1A), but this only represents one of the four scenarios shown in Figure 1.

For cases when v_i is over the ocean and v_{i+6} is inland (Scenario 2; Figure 1B), we observed that nearshore intensification within six hours of landfall could result in underestimation of v_t (e.g., Hurricane Andrew [1992], which intensified in just about three hours from 130 kt at 06:00 UTC to a landfall wind speed of 145 kt at 09:05 UTC). Therefore, we used the exact landfall intensities from the Atlantic Oceanographic and Meteorological Laboratory (AOML 2022). The v_i is replaced by the landfall MSW($v_{t_{LF}}$) except for landfalls from 1971 to 1982, the period for which the Atlantic Hurricane Database Reanalysis Project (Delgado, Landsea, and Willoughby 2018) has yet to be completed. Figure 2 illustrates the v_t during Hurricane Andrew's landfall in 1992 using the given estimation procedure.

For Scenario 3 (Figure 1C) when v_i is over land and v_{i+6} is over the ocean ($v_i > v_{i+6}$), we follow the same procedure as in Scenario 1. In the case of reintensification ($v_i \leq v_{i+6}$), we assumed constant inland MSW ($v_t = v_i$), as the reintensification of TCs is more likely to occur over the ocean than over land. In situations when a TC crosses the peninsula within a six-hour period (v_i and v_t both over the ocean; Scenario 4), we derived v_t by linear interpolation because land interaction is likely minimal.

The v_t values estimated by the four scenarios are then compared to the real-time operational records as archived by the NHC. The NHC issues three-hour intensity updates when tropical storms are near landfall. In more recent years, hourly updates are available for landfalling hurricanes. The MSW is converted to kt from mph (1 mph $\sim$ 0.87 kt) as mph was reported in the NHC operational advisories, whereas kt is used in HURDAT2 and in this study. The number is then rounded to the nearest multiple of five because the MSW in HURDAT2 are reported in 5-kt increments.

Figure 3 compares the v_t with the real-time estimated MSW for recent landfalling named storms and hurricanes after 2000. The estimated v_t aligns well with the real-time estimates, in which the errors generally fall within the uncertainty level (±7 kt) for TCs in the North Atlantic basin after 2000 (Knapp 2019). The goodness of fit is evaluated by R^2 for all paired model and operational estimates, which gives $R^2 = 0.93$. The NHC advisory archives provides intensity changes at short time intervals, but these advisories are based on operational data. Following the hurricane season, NHC conducts a thorough reanalysis of all TCs. As a consequence of this reanalysis, operational advisory intensities might differ from what ends up in HURDAT2. For example, the real-time landfall intensity of Tropical Storm Emily (2017) was assessed at 40 kt but was increased to 50 kt after reassessing Doppler radar in reanalysis (Pasch, Latto, and Cangialosi 2019).

Accumulated Cyclone Energy

This study follows the approach of Truchelut and Staehling (2017), which normalizes ACE by the MSW of interest. We chose 64 kt as the reference MSW so that one ACE unit is equal to a 64 kt Category 1 hurricane on the Saffir-Simpson Hurricane Wind Scale (SSHWS; NOAA 2012) for a six-hour period. Because each v_t represents 0.06 hour temporal resolution, we define an ACE unit as:

$$ACE\ unit = v_t^2/(64^2 \times 100) \quad (3)$$

so that from an energetic perspective, the ACE from a tropical storm at 34 kt is $\sim$ 28 percent of that from a Category 1 hurricane with 64 kt MSW, and a major hurricane at 96 kt is 225 percent of a 64-kt hurricane.

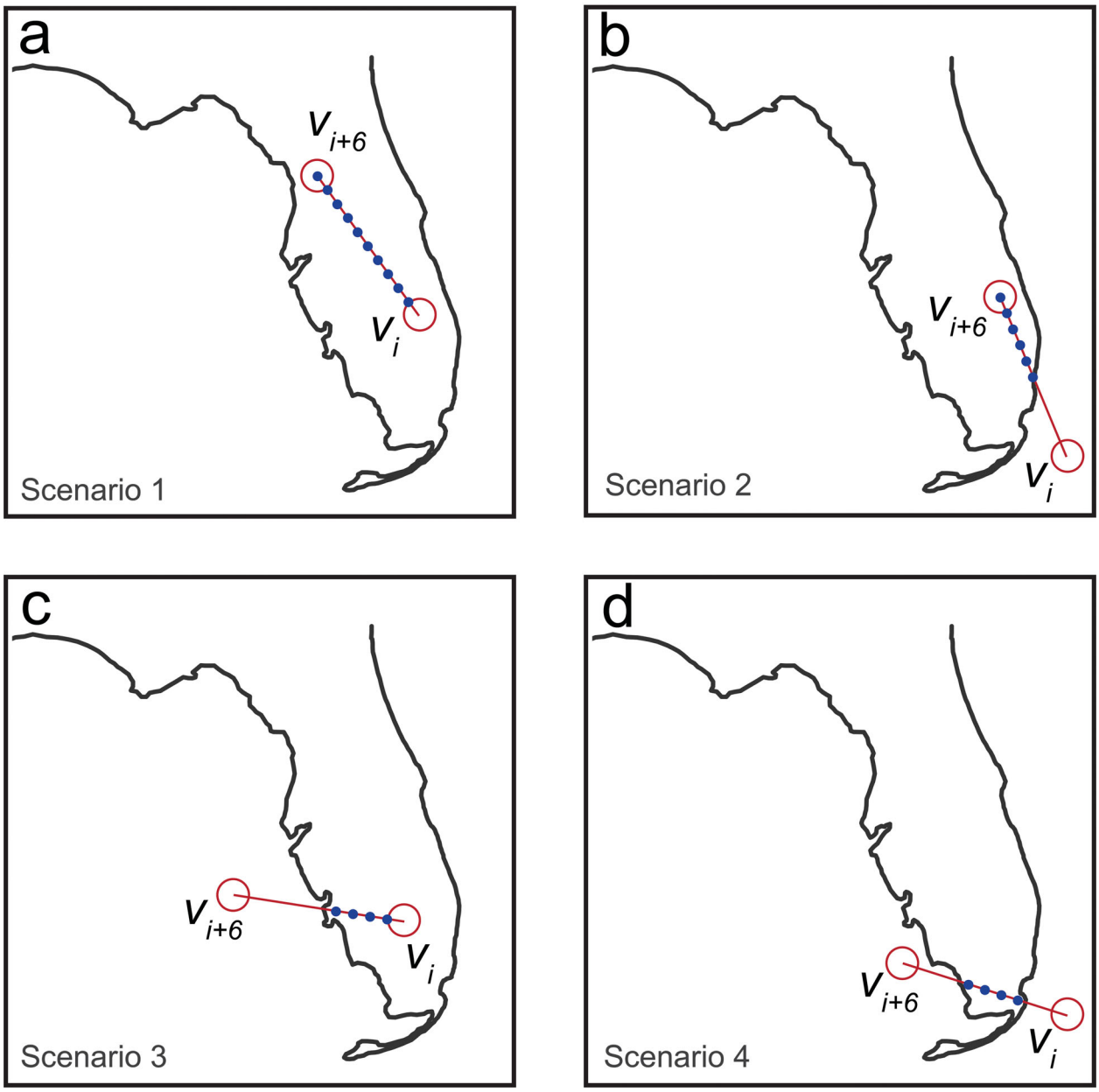

Figure 1. Scenarios used for estimating inland wind decay. Neighboring six-hour track positions are highlighted with circles, and every tenth position of the inland tracks are highlighted with dots. (A) Scenario 1 occurs when the tropical cyclone (TC) is inland for the full six-hour period. (B) Scenario 2 occurs when the TC is over water at the start of the six-hour period and is inland at the end of the six-hour period. (C) Scenario 3 occurs when the TC is over land at the start of the six-hour period and emerges over water by the end of the six-hour period. (D) Scenario 4 occurs when the TC is over water at both the start and end of the six-hour period but crosses land at some point during the six-hour period.

ACE-Based Return Period

By using the ACE unit as our TC metric, for each county in Florida, we first count the years based on the value of $\sum ACE\ unit$. The $\sum ACE\ unit$ describes the sum of ACE, where a value ≥ 0.167 implies an annual TC energetic exposure of the county equivalent to a one-hour occurrence of a Category 1 hurricane. The return period is then calculated by dividing the 121-year record by the number of years that met or exceeded the threshold. Similarly, the return period of energetic exposure equivalent to one hour of a major hurricane (MSW $\geq$ 96 kt, Category 3 in SSHWS) can be derived by setting the threshold of

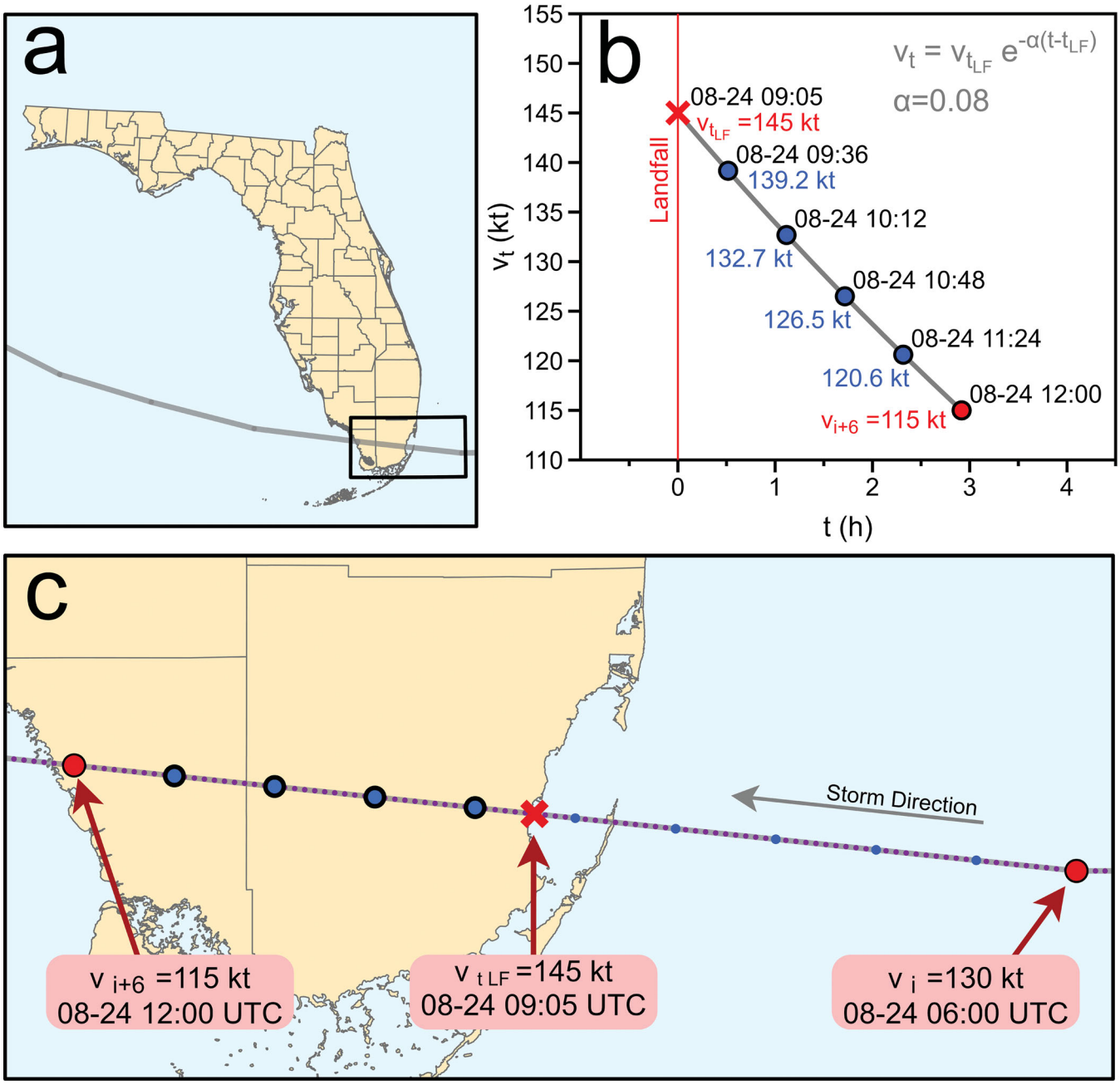

Figure 2. Outline of Hurricane Andrew's landfall in 1992 and our estimation of its intensity crossing the state of Florida. (A) Overview of Hurricane Andrew's track crossing the Florida peninsula. (B) Intensity estimates for Hurricane Andrew from the time of its landfall to the time of its reemergence in the Gulf of Mexico. (C) Enlarged view of the area in the black box from (A). The six-hour track positions are marked with red circles, where the cross represents the landfall location. v_t estimates are illustrated with purple dots, which split the track between the neighboring six-hour position into 100 sections. Every tenth position is marked with purple dots, with those inland highlighted by larger blue circles.

$\sum ACE\ unit \geq 0.375$. As noted, the return period based on an energetic perspective is flexible in indicating the annual risk exposure of a region to TC occurrence. The energetic exposure equivalent to a one-hour major hurricane with $\sum ACE\ unit \geq 0.375$ can also be interpreted approximately as the occurrence of two lower end SSHWS Category 1 (MSW = 64 kt) hurricanes ($\sum ACE\ unit = 0.33$) and one weak tropical storm (MSW = 34 kt; $\sum ACE\ unit = 0.046$). The $\sum ACE\ unit$ generally increases by a

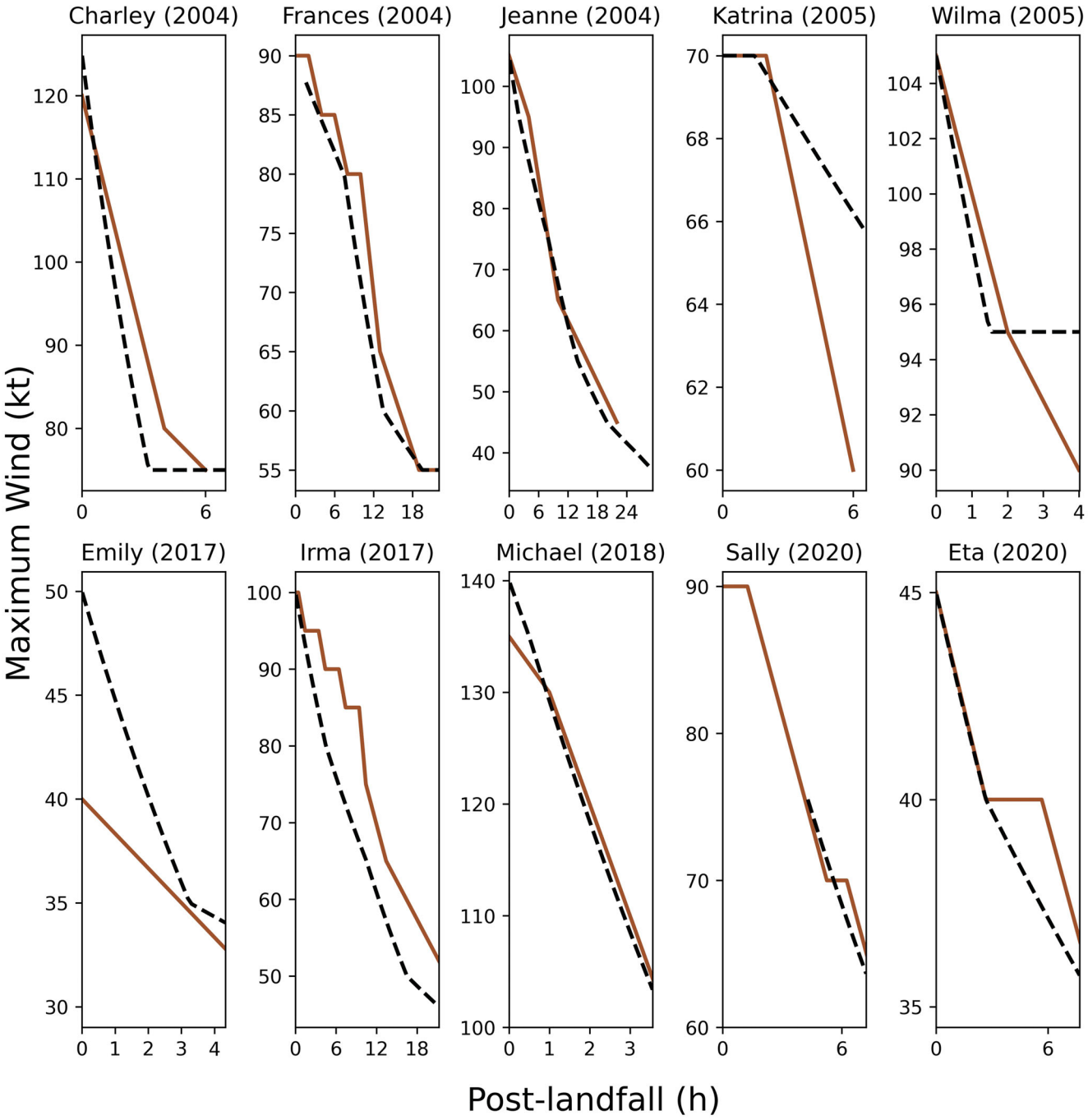

Figure 3. Comparison of the model estimated maximum sustained wind speed (MSW in dashed line) with the real-time operational estimate (in solid line) for selected landfalling tropical cyclones in Florida.

power of two with increasing MSW. Using Polk County in 2004 as an example, three TCs passed over the county (Charley: ~100 minutes with an average MSW of 82 kt; Frances: ~350 minutes with an average MSW of 60 kt; and Jeanne: ~280 minutes with an average MSW of 69 kt), generating a total of ~2.2 $\sum ACE$ *unit*.

Results

Florida Landfalling TC Climatology

Spatially, the frequency of TC strikes is higher along the west coast including the Panhandle compared with the east coast of the peninsula (Figure 4). We used the boundary between Taylor County

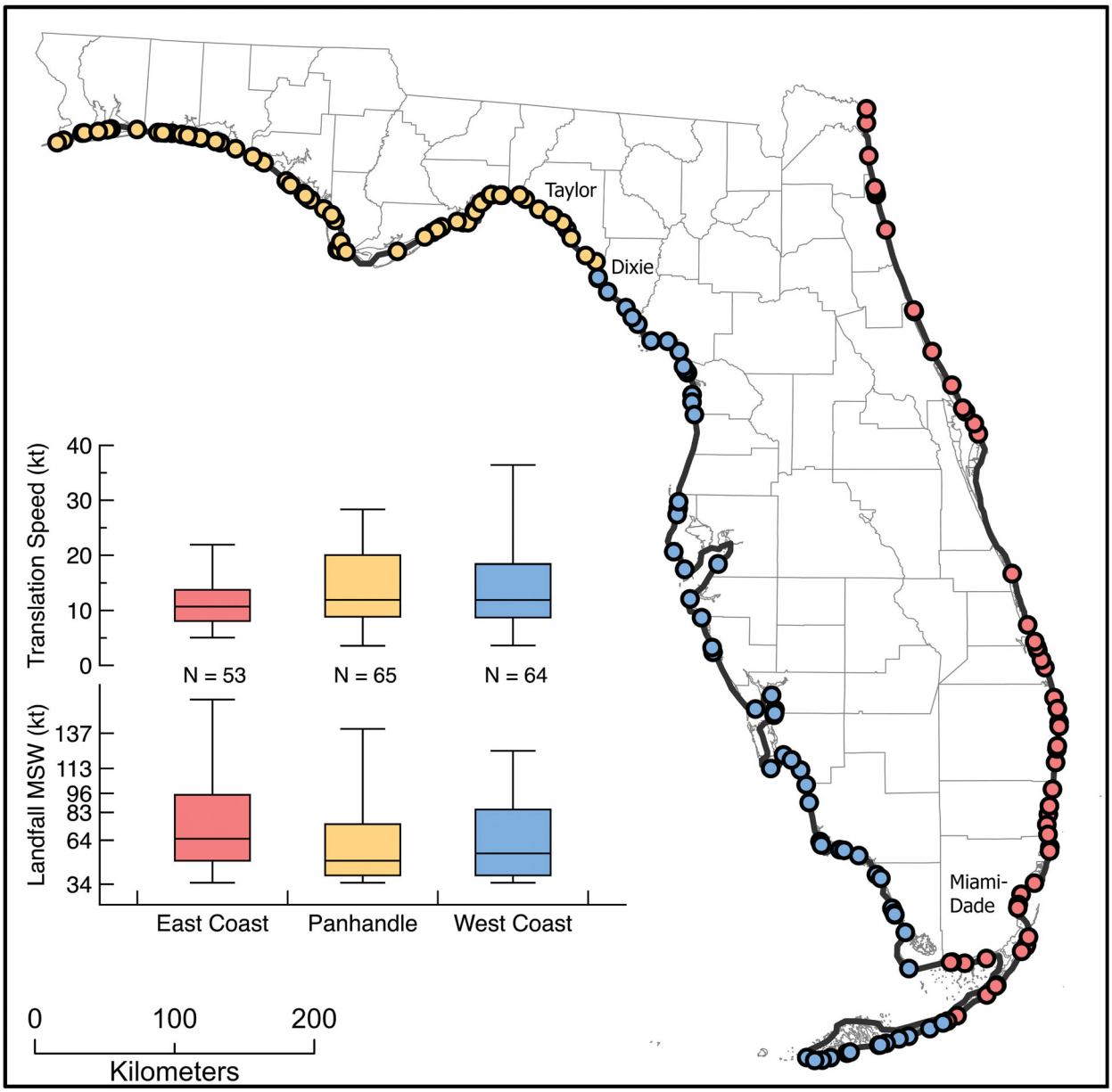

Figure 4. Florida tropical cyclone landfall locations color coded by their landfall region where yellow dots denote Panhandle landfalls, blue dots denote west coast landfalls, and red dots denote east coast landfalls. Also included are box and whisker plots of translation speed and landfall maximum sustained wind speed (MSW).

and Dixie County to distinguish the Panhandle from the west coast and the longitude of 80.85°W (near the west boundary of Miami-Dade County) is employed as the border between the west and east coasts (Zhu, Collins, and Klotzbach 2021b). Historically, storms making landfall along the east coast of Florida tend to be stronger. The lower 25 percent, median, upper 25 percent, and maximum MSW for the east coast of Florida all exceed their corresponding levels for the Panhandle or the west coast of Florida.

Unlike TCs that are mostly making direct landfall along the east and west coasts of Florida (fifty in fifty-three landfall cases and fifty-eight in sixty-four landfall cases, respectively), TC strikes along the Panhandle include landfalls (eleven of sixty-five) that traveled across the peninsula and back to the ocean before making their final landfall (e.g., 1995 Hurricane Erin). Five out of eleven were over the Gulf of Mexico in less than twenty-four hours. The average intensity of their first landfall along the east coast of Florida is 74 kt, and their average MSW still

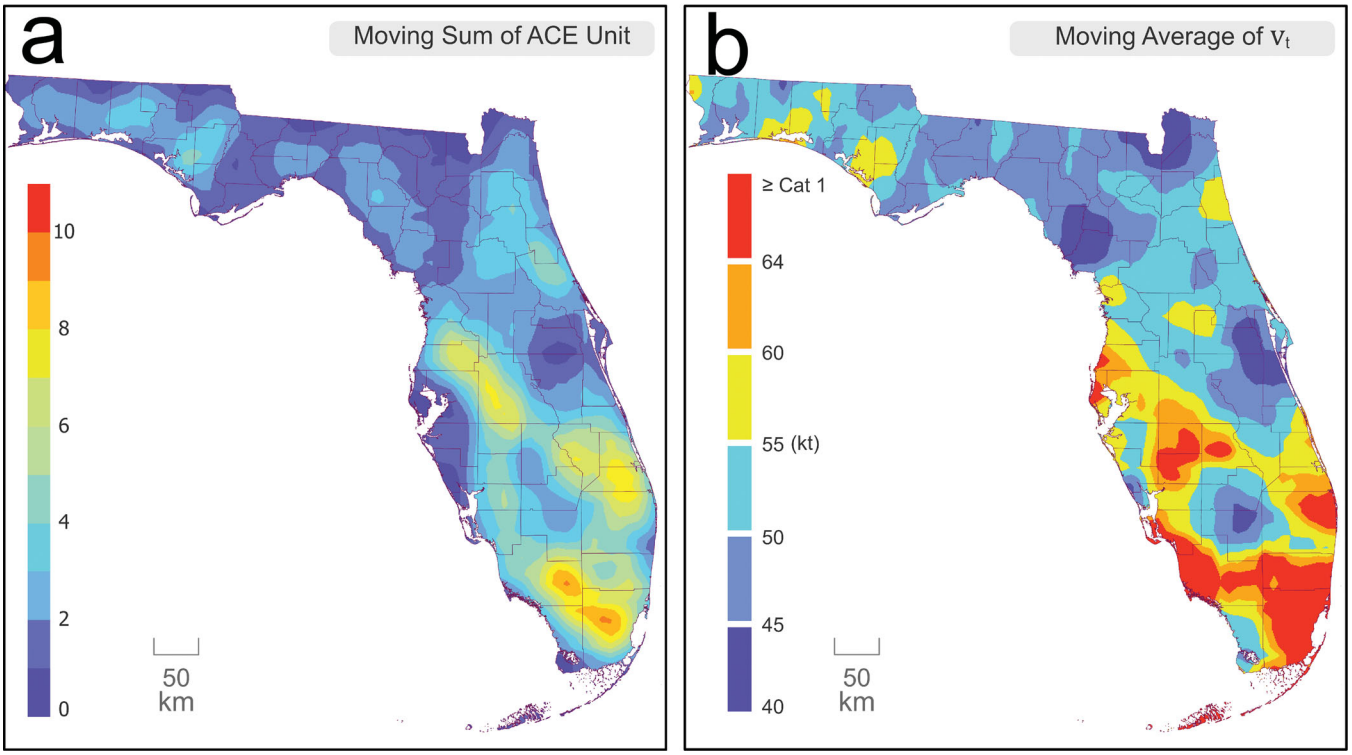

Figure 5. (A) Sum of accumulated cyclone energy (ACE) units in a moving 50×50 km catchment with the original 10×10 km resolution bilinearly resampled to 1×1 km for better visualization purpose. (B) As in (A) but for a moving average of the estimated inland maximum sustained wind speed (v_t).

remained ~52 kt when striking the Panhandle (not shown in Figure 4). This implies that land impacts on these storms were relatively weak. The translation speed during the six-hour time window at landfall (between the first inland track point and the last track point over the ocean) shows similar median levels for each part of the Florida coastline, but east coast landfalls have relatively less spread, with most landfalling TCs having a translation speed of ~10 kt. It is worth noting that the average forward speed of TCs making their second landfall in the Panhandle is relatively slow (~10 kt, not shown in Figure 4), allowing TCs to gain sufficient energy from warm waters in the northeastern Gulf of Mexico.

Spatial Distribution of ACE Units

Because TC intensity sometimes changes little while transiting Florida, we next focus on inland TC intensity. The frequency and intensity of TCs by $\sum ACE\ unit$ is derived by a moving 50×50 km area based on the median of the available RMW (55.6 km TCs over Florida and 46.3 km for TCs that reached hurricane intensity). The calculation is based on the Extended Best Track database that has data available since 1988 (Demuth, DeMaria, and Knaff 2006). The output cell size was set to 10×10 km to account for the 0.1° (~10 km) track uncertainties from the TC data source. Because ACE describes total energetic exposure, areas with higher values imply more frequent TCs, or greater MSW, from each TC (Figure 5A).

The southeast coast and central Florida have exhibited the largest exposure to TCs in the state over the past 121 years, with $\sum ACE\ unit \geq 6$ in most of these areas. As noted earlier, the sum of the ACE unit provides a total exposure of one area to TC wind risk. Hence, one interpretation could be that in the preceding 121 years, the total TC wind that passed over an area within a 2,500 km^2 catchment is equivalent to at least thirty-six hours of SSHWS Category 1 hurricane or higher. We note that although the moving sum of the ACE unit is a good indicator for highlighting areas with high levels of TC activity, coastal regions might be misinterpreted due to errors at the margins. Figure 5B, as a supplement to Figure 5A, describes the average v_t in

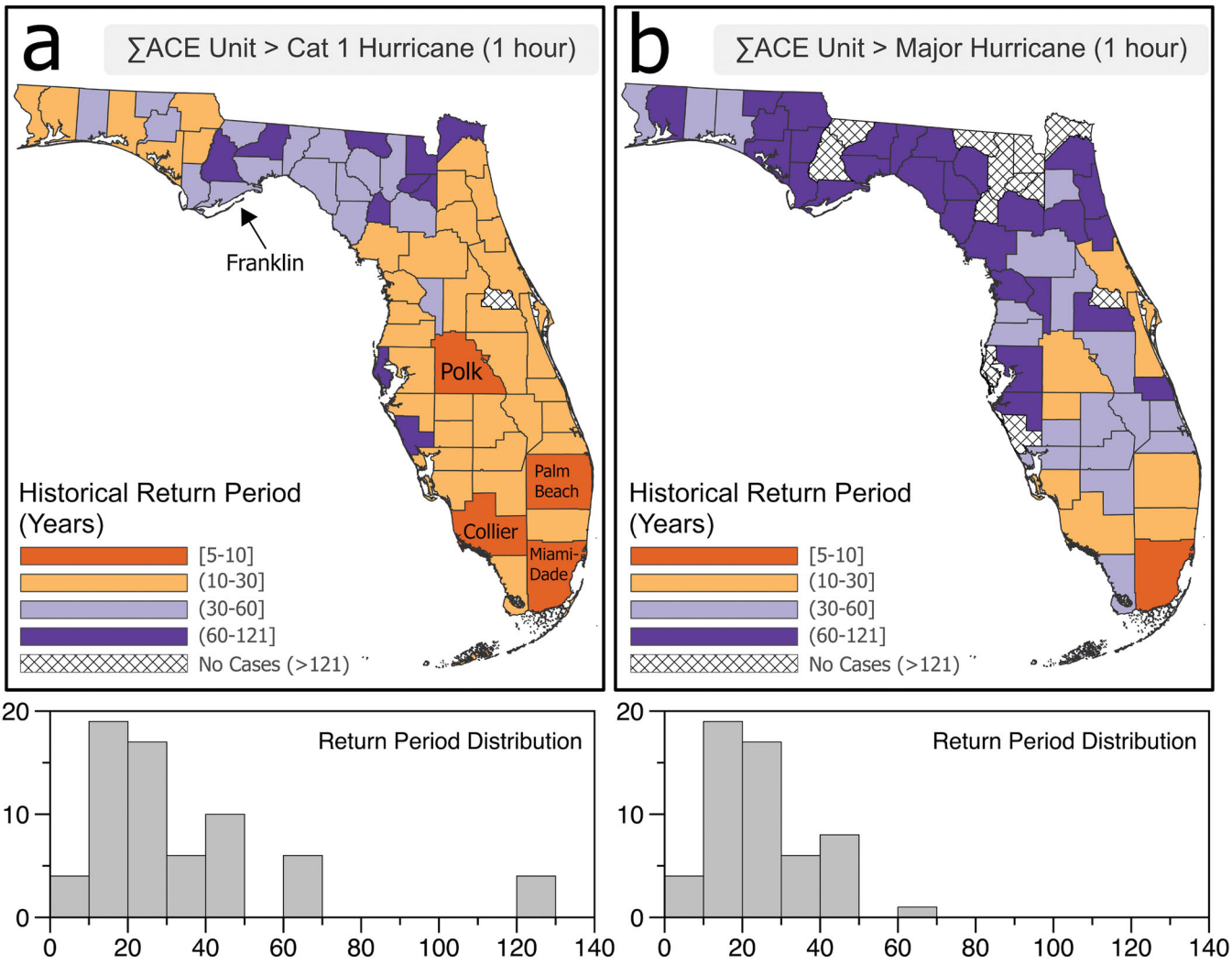

Figure 6. County-level return period based on the sum of the accumulated cyclone energy (ACE) unit and its distribution. (A) Equivalent to a hurricane strike with an intensity level of at least Saffir-Simpson Hurricane Wind Scale (SSHWS) Category 1 that is maintained for one hour. (B) As in (A) but for SSHWS Category 3 and above.

a moving 50 × 50 km box. In Tampa Bay, for example, the occurrence of TCs is not as frequent as seen on the southeast coast, but the average MSW from both regions exceeds the SSHWS Category 1 threshold. In general, counties along the west coast are less exposed to intense hurricane strikes compared to the east coast. This agrees with previous studies on spatial return periods (R. A. Muller and Stone 2001; Keim, Muller, and Stone 2007).

ACE-Based Return Periods

At the county level, the ACE-based return period reflects the frequency of annual accumulated TC wind with an ACE equivalent to one hour of hurricane wind $\geq$ 64 kt (Figure 6A), or a major hurricane $\geq$ 96 kt (Figure 6B). The majority of counties in central and South Florida and the west Panhandle regions of the state are expected to receive annual ACE greater than a sustained one-hour Category 1 hurricane wind every ten to thirty years. Polk, Collier, Palm Beach, and Miami-Dade counties are at the top of the list with a less than ten-year return period. With a more intense threshold applied (annual ACE greater than a one-hour Category 3 hurricane), Miami-Dade County has the highest return period, with most of the rest of southern Florida, the central part of the east coast of Florida, and inland central Florida having less than a thirty-year return period. The Big Bend region has

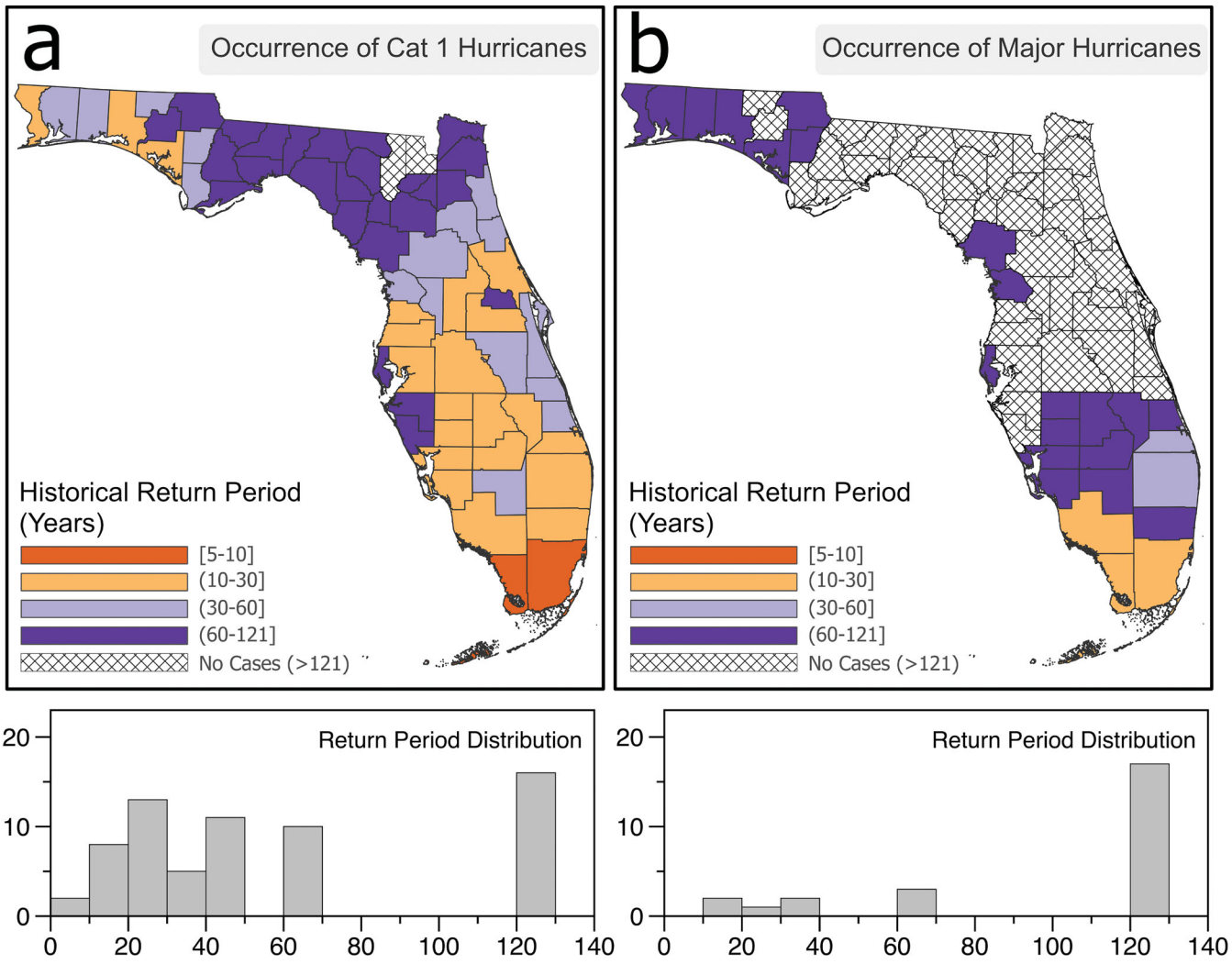

Figure 7. Track-based county-level return period and its distribution. (A) For an occurrence of Category 1 hurricane and above (≥ 64 kt). (B) As in (A) but for Category 3 hurricane and above (≥ 96 kt).

relatively low exposure to TC wind risk due to relatively weaker TCs over the region (Figure 5B), especially those that move from south to north across Florida, which have likely weakened considerably by the time that they approach the Big Bend region.

As previously mentioned, because ACE describes both TC duration and intensity, counties with higher ACE exposure could be due to more frequent occurrences of TCs, more intense TCs, or both. Figure 7 displays the return period by only considering years with an occurrence of v_t >64 kt (Figure 7A) and > 96 kt (Figure 7B). Similar to the pattern from the ACE-based return period, northern and west-central Florida see the least frequent hurricane strikes in the state, whereas the southern portion of the state typically has the most. By comparing the return period based on ACE unit and MSW, it is worth noting that for Polk County, although we see a return period in the ten- to thirty-year category for the annual sum of an ACE unit that is equivalent to a major hurricane, there have been no major hurricanes in the county. This implies that the return period from the ACE approach does not necessarily indicate intense TC strikes but could also imply frequent occurrences or long duration of weaker TCs over the county.

Discussion

The general spatial patterns of TC risks for coastal communities are in line with the results from earlier studies but show more conservative estimates. Keim,

Muller, and Stone (2007) suggested the shortest return period of TC landfall occurred in South Florida, with Miami Beach, Palm Beach, and Key Largo having return periods of hurricane strikes under five years. The Florida Panhandle sees a less than ten-year return period, and Tampa Bay is estimated at twenty-six years. These return periods are shorter than those estimated by this study. The discrepancies can be explained by two factors. First, we only included the number of years, such as whether the annual accumulated ACE unit surpasses the ACE that is equivalent to a one-hour sustained hurricane wind (Figure 6A) or whether there is a hurricane landfall in a given year (Figure 7A). By comparison, Keim, Muller, and Stone (2007) considered each landfalling hurricane as a separate case, resulting in more occurrences to be counted during years with multiple landfall hurricane landfall events. Second, we only considered direct landfall events in which the storm center was over land. Keim, Muller, and Stone (2007) applied the uniform intensity–storm size model of Pielke and Pielke (1997) so that nearshore hurricanes, either within a distance parallel to the coast or those with hurricane intensity offshore but decaying to a tropical storm at landfall (<64 kt), were all counted in the return period calculation for the occurrence of hurricane strikes in coastal cities. We agree that, by including the storm size together with the MSW, the exposure of coastal communities to hurricane risks could be better represented (Zhai and Jiang 2014). Because the actual storm size varies on a case-by-case basis and the storm size changes after landfall, implementing a uniform storm size model in our case could lead to large uncertainties, especially for inland regions. To test the sensitivity of the location of the storm MSW, we performed a random perturbation of 20 km and 50 km of radius to the six-hour best-track and reran the analysis for the return period of the sum of ACE units that are equivalent to an hour of SSHWS Category 1 hurricane exposure (Figure 8). With random perturbations applied to TC locations, nearshore storms that did not make landfall, such as Hurricane Matthew (2016), might now be included. The perturbation adds small uncertainties but the overall spatial patterns remain similar to the results from the observed data.

Malmstadt, Elsner, and Jagger (2010) applied a 100-km radius around the centroid of Florida's major cities and gave a shorter return period given the same wind level. By comparison, with the same 100-km radius applied but using a synthetic TC data set equivalent to about 10,000 years of hurricanes, Bloemendaal et al. (2020) found an approximately ten-year return period for a SSHWS Category 1 hurricane in Miami, which is similar to the derived return period from both ACE and MSW in this study but without considering the inland TC durations in Florida at the county level.

The return period for TC wind risks can be estimated by historical data or by a combination of data and statistical models (Malmstadt, Elsner, and Jagger 2010), but the calculations are somewhat limited by the data that are available. The HURDAT2 database currently extends back about 170 years for the Atlantic basin, with the accuracy of TC intensity and location improving with time with more advanced monitoring technologies and denser inland observation stations (Vecchi et al. 2021). One potential way to extend hurricane landfall data farther back in time is through the use of paleotempestology (Donnelly et al. 2001; J. Muller et al. 2017; Cerrito, Mock, and Collins 2021).

Several paleotempestology studies from Florida indicate return periods different from those presented in this article. Paleotempestology-derived return periods from Mullet Pond in Franklin County, located on the Florida Panhandle, indicate an average of 3.9 storms per century on a 4,500-year overwash record (Lane et al. 2011). From the track-based record between 1900 and 2020, Franklin County only received one direct landfall event that was over SSHWS Category 1 in the past 121 years (~0.83 per century), with three years (~2.5 per century) that contributed to the annual ACE equivalent to a one-hour Category 1 hurricane. By comparison, the 1,000-year paleotempestology derived return periods from Island Bay, near Naples, in Collier County in southwest Florida, suggest 0.9 high-threshold events (potentially from hurricanes with SSHWS Category 3 and above) per century (Ercolani et al. 2015). The corresponding event frequencies in the post-1900 portion of the sediment record were two high-threshold events per century. This estimate agrees with the wind-based return period (Figure 7B) but is lower than the ACE-based return period from this study (Figure 6B). Therefore, the paleotempestology record does indicate higher high-threshold storm return periods along the Panhandle than that seen in southwest Florida, where ACE-based return periods would indicate a higher occurrence of high-threshold events for southwest Florida than for the Florida Panhandle.

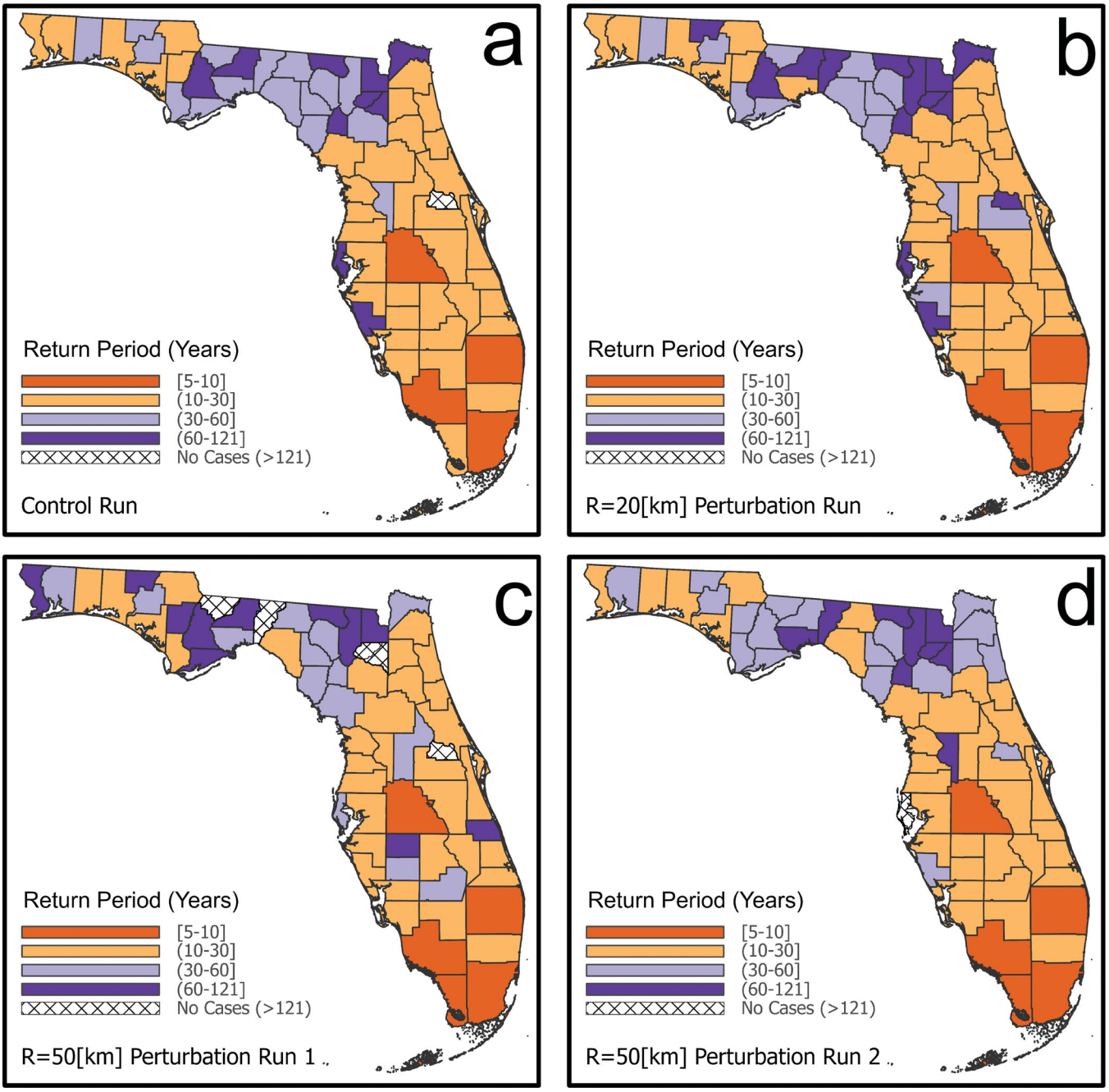

Figure 8. Sensitivity test runs for Figure 6A (the return period of tropical cyclone [TC] activities equivalent to the exposure of one-hour Category 1 hurricane) with random perturbations of storm locations applied. (A) Control run. (B) R = 20 [km] perturbation run. (C) R = 50 [km] perturbation run 1. (D) R = 50 [km] perturbation run 2.

Discrepancies between the return periods derived from paleotempestology and the modern track-based data (1900–2020) are likely due to how TC signals are detected. Because paleotempestology relies on storm surge (J. Muller et al. 2022), whereas the ACE-based approach depends on inland wind speed, TC return periods for inland regions are not suitable for comparisons between the two approaches. It is also important to note that the hurricane-deposited signature can vary from site to site, depending on the hurricane's duration and intensity, the site's position relative to the landfall location, the influence of local coastal geomorphology, and the integrity of preservation of the hurricane signature. Some studies find that paleotempestology archives often record more intense events with greater storm surge (e.g., Liu and Fearn

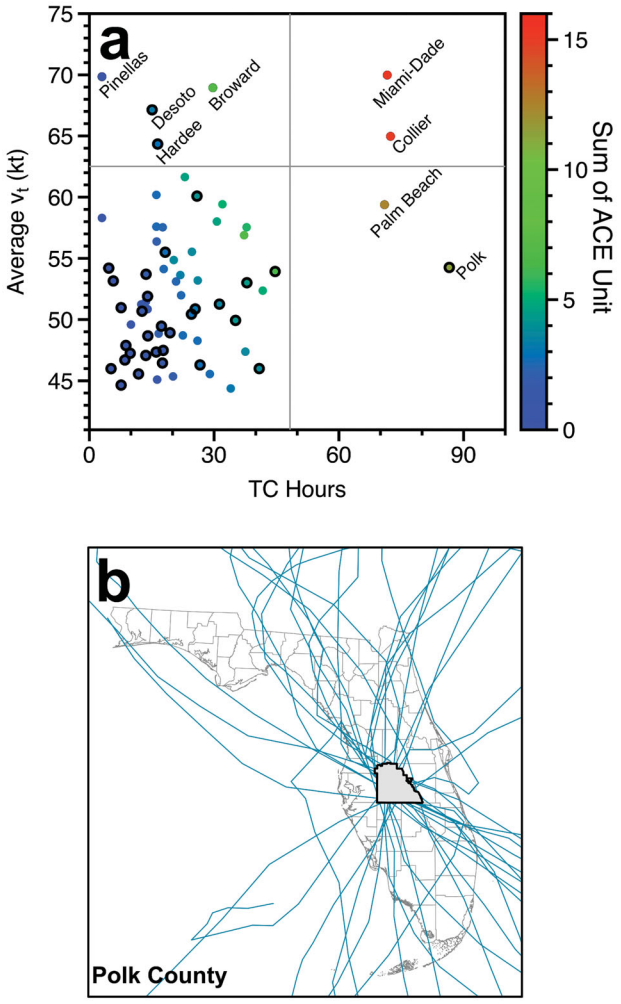

Year	Storm Name in (b)	TC Hours	Avg. v_t (kt)
1909	Tropical Storm Three	7.3	35
1910	Cuba Hurricane	5.2	64
1916	Tropical Storm One	7.0	38
1928	Fort Pierce Hurricane	5.9	44
1928	Okeechobee Hurricane	3.6	84
1933	Treasure Coast Hurricane	4.4	62
1939	Hurricane Two	3.2	52
1945	Homestead Hurricane	4.2	72
1949	Florida Hurricane	2.8	72
1950	EASY	1.8	57
1950	KING	0.8	76
1960	DONNA	4.1	71
1960	FLORENCE	0.6	34
1968	ABBY	3.0	45
1984	ISIDORE	6.1	45
1988	KEITH	2.5	39
1995	ERIN	2.7	53
1995	JERRY	3.7	35
2001	GABRIELLE	4.5	45
2004	CHARLEY	1.7	82
2004	FRANCES	5.9	60
2004	JEANNE	4.7	79
2017	IRMA	0.7	70

Official naming system for tropical storms in Atlantic basin started in 1950

Figure 9. (A) Distribution of tropical cyclone (TC) duration and average estimated wind speed for all sixty-seven Florida counties with total accumulated cyclone energy (ACE) depicted. Inland counties are marked with bold outlines. The gray lines (both horizontal and vertical) represent the threshold of 1.5 standard deviations from the mean. (B) Tracks of TCs that struck Polk County between 1900 and 2020. The table lists the year, name, TC hours, and average maximum sustained wind speed for the TCs displayed in (B).

1993, 2000; Donnelly et al. 2001; Donnelly and Woodruff 2007; Brandon et al. 2013; van Hengstum et al. 2014). Lower category storms, however, such as those that are larger in size and moving with a slower forward speed, can produce significant storm surge, thereby overwashing barrier islands and depositing storm layers (Hawkes and Horton 2012; Williams and Denlinger 2013; Lin et al. 2014).

Whereas each v_t represents 3.6 minutes (six hours/100) of TC occurrences, the total number of v_t reflects the duration of all TCs within each county (e.g., TC hours). Counties with higher calculated TC hours could be due to more frequent TC strikes, or slower moving TCs. Figure 9A depicts the spread of all sixty-seven Florida counties in terms of the total TC duration, averaged v_t, and $\sum ACE\ unit$. Counties with TC hours or averaged v_t greater than or less than 1.5 standard deviations from the mean are labeled. Miami-Dade and Collier are two South Florida coastal counties with the highest ACE exposure due to both a high frequency of TC occurrences and intense TC strikes with averaged in-county v_t above SSHWS Category 1 ($\geq$ 64 kt). Although coastal counties dominate high ACE exposure, Polk County, as mentioned earlier, had the highest amount of TC hours across the state, making it an intersection point for TCs tracking across Florida from either the Gulf of Mexico or the North Atlantic (Figure 9B; inland counties are marked with a bold outline). In 2004 alone, three SSHWS Category 1 hurricanes (table in Figure 9) struck Polk County in less than two months. Because TCs are expected to quickly weaken after landfall due

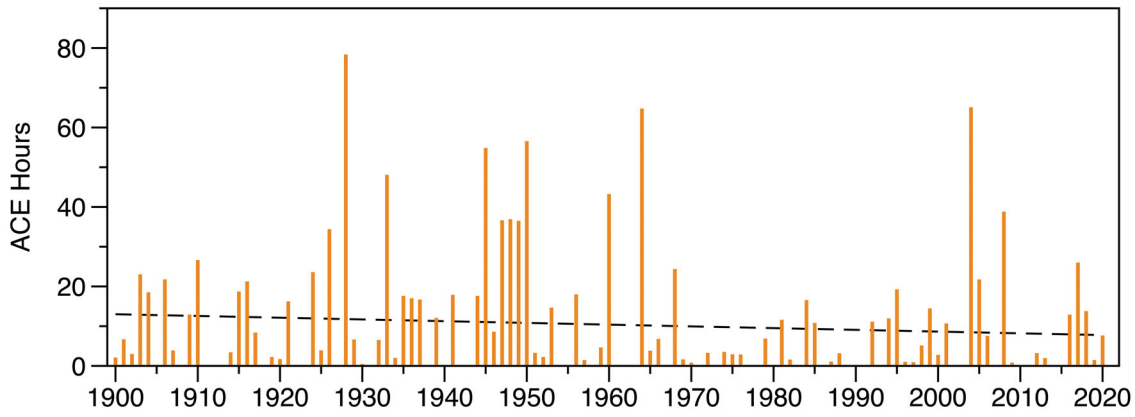

Figure 10. Tropical cyclone activities in Florida as represented by accumulated cyclone energy (ACE) hours. One ACE unit can be interpreted as a 1-hour exposure to 64-kt wind or about 3.5 hours exposure to 34-kt wind.

to the loss of the storm's primary energy source (e.g., the warm ocean), the observed high v_t (Figures 5B and 7A) for inland Florida counties, especially in the southern part of the state, deserves special attention. Here, relatively weak TC postlandfall decay due to potentially sufficient latent heat flux (Andersen and Shepherd 2017), moisture supply from the Everglades (Hlywiak and Nolan 2021), as well as some portion of the TCs (especially large TCs) remaining over the ocean (DeMaria, Knaff, and Kaplan 2006) is important to recognize.

Limitation and Future Works

This study examines TC activity in Florida between 1900 and 2020 and reveals exposure frequency for various counties in the state, but there are several limitations of this study that should be noted. The first is that ACE only considers the track point as an indicator of the spatial location of the TC MSW. In the real world, the area of destructive winds can extend more than 100 km away from the center. Both the RMW and the four-quadrant average radius of 34 kt (R34) wind can serve as a good approximation for the area exposed to TCs. The Extended Best Track database (Demuth, DeMaria, and Knaff 2006) provides RMW and R34 for each storm back to 1988, but R34 was not reanalyzed until 2004, and RMW was not reanalyzed during our study period. Consequently, R34 from 1988 to 2003 and RMW from 1988 to 2020 are from operational estimates. With both quantities now being reanalyzed, integrated kinetic energy (IKE) can be employed as an alternative way of assessing the TC damage potential along the U.S. coast (Powell and Reinhold 2007; Misra, DiNapoli, and Powell 2013), particularly along the Atlantic East Coast. IKE has served as a better predictor of hurricane damage than MSW for landfalls from Georgia to Maine but not for lower latitude landfalls from Texas to Florida (Klotzbach et al. 2022). In addition, TC winds are only one part of the TC risk, as storm surge and torrential rainfall are also important parameters to consider for future studies when composing a comprehensive return period of TC risks for the region of interest (Zhou et al. 2018; Chin et al. 2019).

Temporal variations should also be considered when analyzing TC return periods from historical records. Figure 10 shows annual accumulated ACE hours in Florida from 1900 to 2020. One unit of ACE hours represents an hour of wind exposure equivalent to 64 kt. TC activity in Florida during the second half of the 121-year period is generally quieter, especially during 1970 to 2000, when compared to the first half from 1900 to 1960, although the long-term downward trend is not significant (slope: -0.05 ± 0.08). Therefore, the estimated return period can be influenced by the time window selected. Studies choosing only 1970 to 2020 as the reference period for TC occurrences could result in longer return periods when compared to the 121-year record. Future studies are encouraged to regularly update return periods to reflect temporal variations and changes in TC activity in a changing climate.

Conclusion

This research uses ACE as an approach to derive the historical return period for TCs in Florida. An algorithm for estimating TC inland wind between

the six-hour track points is introduced. The algorithm covers different scenarios that could occur when either of the six-hour track points is not over land. The ACE-based return period reflects strong TC occurrences but also examines the total annual exposure of a region to TC wind. The majority of central and South Florida are expected to experience an ACE equivalent of at least one-hour exposure to a SSHWS Category 1 hurricane with a return period of less than thirty years. The expected short TC return period shown in southeast Florida is mainly due to the intensity of the storms making landfall there. The ACE-based return period, however, also reveals a high clustering of TC wind duration in central Florida, especially in Polk County.

The general pattern of the ACE-based return period across the Florida peninsula agrees with the existing modern track-based literature but shows variations caused by the different methods applied. Examples include taking a fixed hurricane radius into consideration for the wind impact (Keim, Muller, and Stone 2007) or using a city-oriented search radius (Malmstadt, Elsner, and Jagger 2010) rather than county-based as used in this study.

By comparing the results with paleotempestology-derived return periods, the ACE-based approach suggests a longer return period for TCs than the paleotempestology approach for the Florida Panhandle. Because long-term paleotempestological records are created using the preserved hurricane overwash signature from storm surge as a hurricane nears the coast, it is more sensitive to TC-induced storm surge rather than TC intensity by itself. This is likely the major cause for different return period estimates derived from the wind-based ACE and the storm-surge-based paleotempestology data.

Because the primary analysis of this study is conducted on the ArcGIS platform, it can benefit geographers from different disciplines, or professionals using ArcGIS in the insurance industry and operational agencies that are interested in integrating inland TC wind risk into their specific projects.

Acknowledgments

The authors would like to thank two anonymous reviewers and the editor for helpful comments that improved the article.

Disclosure Statement

No potential conflict of interest was reported by the authors.

Funding

This work was supported by the Florida Sea Grant Program (Project R/C-S-65). Philip Klotzbach would like to acknowledge a grant from the G. Unger Vetlesen Foundation.

ORCID

Yi-Jie Zhu http://orcid.org/0000-0001-7828-9148

Data Availability Statement

All original data used in this study are publicly available. The TC data were obtained from the International Best Track Archive for Climate Stewardship version 4 (IBTrACS; https://www.ncdc.noaa.gov/ibtracs/index.php?name=ib-v4-access). The TC landfall data are from the Atlantic Oceanographic and Meteorological Laboratory (AOML; https://www.aoml.noaa.gov/hrd/hurdat/UShurrs_detailed.html). The ArcGIS-Python code is available on https://github.com/zhu-yijie-geo/py_gis.git.

References

Andersen, T., and M. Shepherd. 2017. Inland tropical cyclones and the "brown ocean" concept. In *Hurricanes and climate change*, ed. J. M. Collins and K. Walsh, 117–34. Berlin, Germany: Springer. doi: 10.1007/978-3-319-47594-3_5.

Atlantic Oceanographic and Meteorological Laboratory (AOML). 2022. Detailed list of continental United States hurricane impacts/landfalls 1851–1970, 1983–2021. Accessed May 4, 2022. https://www.aoml.noaa.gov/hrd/hurdat/UShurrs_detailed.html.

Bell, G. D., M. S. Halpert, R. C. Schnell, R. W. Higgins, J. Lawrimore, V. E. Kousky, R. Tinker, W. Thiaw, M. Chelliah, and A. Artusa. 2000. Climate assessment for 1999. *Bulletin of the American Meteorological Society* 81 (6):S1–S50. doi: 10.1175/1520-0477(2000)81[s1:CAF]2.0.CO;2.2.0.CO;2

Blake, E. S., C. W. Landsea, and E. J. Gibney. 2011. The deadliest, costliest, and most intense United States tropical cyclones from 1851 to 2010 (and other frequently requested hurricane facts). NOAA/National Weather Service, National Centers for

Environmental Prediction, National Hurricane Center. Accessed May 4, 2022. https://repository.library.noaa.gov/view/noaa/6929.

Blake, E. S., E. N. Rappaport, and C. W. Landsea. 2007. The deadliest, costliest, and most intense United States tropical cyclones from 1851 to 2006 (and other frequently requested hurricane facts). NOAA/National Weather Service, National Centers for Environmental Prediction, National Hurricane Center. Accessed May 4, 2022. https://www.nhc.noaa.gov/pdf/nws-nhc-6.pdf.

Bloemendaal, N., H. De Moel, S. Muis, I. D. Haigh, and J. C. Aerts. 2020. Estimation of global tropical cyclone wind speed probabilities using the STORM dataset. *Scientific Data* 7 (1):1–11. doi: 10.1038/s41597-020-00720-x.

Brandon, C. M., J. D. Woodruff, D. P. Lane, and J. P. Donnelly. 2013. Tropical cyclone wind speed constraints from resultant storm surge deposition: A 2500 year reconstruction of hurricane activity from St. Marks, FL. *Geochemistry, Geophysics, Geosystems* 14 (8):2993–3008. doi: 10.1002/ggge.20217.

Cerrito, E. L., C. J. Mock, and J. M. Collins. 2021. The Great Havana Hurricane of 1846: A reconstruction of the storm's track, intensity, and impacts. *Annals of the American Association of Geographers* 111 (6):1–17. doi: 10.1080/24694452.2020.1838257.

Chin, D. A., M. A. Jacketti, N. S. Karpathy, and P. J. Sahwell. 2019. Accounting for tropical cyclones in extreme rainfall distributions in Florida. *Journal of Hydrologic Engineering* 24 (11):05019028. doi: 10.1061/(ASCE)HE.1943-5584.0001858.

Collins, J. M., and D. R. Roache. 2017. The 2016 North Atlantic hurricane season: A season of extremes. *Geophysical Research Letters* 44 (10):5071–77. doi: 10.1002/2017GL073390.

Delgado, S., C. W. Landsea, and H. Willoughby. 2018. Reanalysis of the 1954–63 Atlantic hurricane seasons. *Journal of Climate* 31 (11):4177–92. doi: 10.1175/JCLI-D-15-0537.1.

DeMaria, M., J. A. Knaff, and J. Kaplan. 2006. On the decay of tropical cyclone winds crossing narrow landmasses. *Journal of Applied Meteorology and Climatology* 45 (3):491–99. doi: 10.1175/JAM2351.1.

Demuth, J. L., M. DeMaria, and J. A. Knaff. 2006. Improvement of advanced microwave sounding unit tropical cyclone intensity and size estimation algorithms. *Journal of Applied Meteorology and Climatology* 45 (11):1573–81. doi: 10.1175/JAM2429.1.

Done, J. M., K. M. Simmons, and J. Czajkowski. 2018. Relationship between residential losses and hurricane winds: Role of the Florida building code. *ASCE-ASME Journal of Risk and Uncertainty in Engineering Systems, Part A: Civil Engineering* 4 (1):04018001. doi: 10.1061/AJRUA6.0000947.

Donnelly, J. P., S. Smith Bryant, J. Butler, J. Dowling, L. Fan, N. Hausmann, P. Newby, B. Shuman, J. Stern, K. Westover, et al. 2001. 700 yr sedimentary record of intense hurricane landfalls in southern New England. *Geological Society of America Bulletin* 113 (6):714–27. doi: 10.1130/0016-7606(2001)113%3C0714:YSROIH%3E2.0.CO;2.

Donnelly, J. P., and J. D. Woodruff. 2007. Intense hurricane activity over the past 5,000 years controlled by El Niño and the West African monsoon. *Nature* 447 (7143):465–68. doi: 10.1038/nature05834.

Ercolani, C., J. Muller, J. Collins, M. Savarese, and L. Squiccimara. 2015. Intense southwest Florida hurricane landfalls over the past 1000 years. *Quaternary Science Reviews* 126:17–25. doi: 10.1016/j.quascirev.2015.08.008.

Federal Emergency Management Agency (FEMA). 2005. Mitigation assessment team report: Hurricane Charley in Florida. Observations, recommendations, and technical guidance. Accessed June 3, 2022. https://www.fema.gov/sites/default/files/2020-08/fema488_mat_report_hurricane_charley_fl.pdf.

Hall, T. M., and J. P. Kossin. 2019. Hurricane stalling along the North American coast and implications for rainfall. *NPJ Climate and Atmospheric Science* 2 (1):1–9. doi: 10.1038/s41612-019-0074-8.

Hawkes, A. D., and B. P. Horton. 2012. Sedimentary record of storm deposits from Hurricane Ike, Galveston and San Luis Islands, Texas. *Geomorphology* 171–72:180–89. doi: 10.1016/j.geomorph.2012.05.017.

Hlywiak, J., and D. S. Nolan. 2021. The response of the near-surface tropical cyclone wind field to inland surface roughness length and soil moisture content during and after landfall. *Journal of the Atmospheric Sciences* 78 (3):983–1000. doi: 10.1175/JAS-D-20-0211.1.

Jagger, T. H., and J. B. Elsner. 2006. Climatology models for extreme hurricane winds near the United States. *Journal of Climate* 19 (13):3220–36. doi: 10.1175/JCLI3913.1.

Jagger, T. H., and J. B. Elsner. 2012. Hurricane clusters in the vicinity of Florida. *Journal of Applied Meteorology and Climatology* 51 (5):869–77. doi: 10.1175/JAMC-D-11-0107.1.

Kaplan, J., and M. DeMaria. 1995. A simple empirical model for predicting the decay of tropical cyclone winds after landfall. *Journal of Applied Meteorology* 34 (11):2499–2512. doi: 10.1175/1520-0450(1995)034<2499:ASEMFP>2.0.CO;2.

Keim, B. D., R. A. Muller, and G. W. Stone. 2007. Spatiotemporal patterns and return periods of tropical storm and hurricane strikes from Texas to Maine. *Journal of Climate* 20 (14):3498–3509. doi: 10.1175/JCLI4187.1.

Klotzbach, P. J., M. M. Bell, S. G. Bowen, E. J. Gibney, K. R. Knapp, and C. J. Schreck, III. 2020. Surface pressure a more skillful predictor of normalized hurricane damage than maximum sustained wind. *Bulletin of the American Meteorological Society* 101 (6):E830–E846. doi: 10.1175/BAMS-D-19-0062.1.

Klotzbach, P. J., D. R. Chavas, M. M. Bell, S. G. Bowen, E. J. Gibney, and C. J. Schreck, III. 2022. Characterizing continental US hurricane risk: Which intensity metric is best? *Journal of Geophysical Research: Atmospheres* 127 (18):e2022JD037030.

Klotzbach, P. J., C. J. Schreck III, J. M. Collins, M. M. Bell, E. S. Blake, and D. Roache. 2018. The extremely active 2017 North Atlantic hurricane season. *Monthly Weather Review* 146 (10):3425–43. doi: 10.1175/MWR-D-18-0078.1.

Knapp, K. R. 2019. International Best Track Archive for Climate Stewardship (IBTrACS) technical documentation. Accessed October 10, 2022. https://www.ncei.noaa.gov/sites/default/files/2021-07/IBTrACS_version4_Technical_Details.pdf.

Knapp, K. R., M. C. Kruk, D. H. Levinson, H. J. Diamond, and C. J. Neumann. 2010. The International Best Track Archive for Climate Stewardship (IBTrACS) unifying tropical cyclone data. *Bulletin of the American Meteorological Society* 91 (3):363–76. doi: 10.1175/2009BAMS2755.1.

Kossin, J. P. 2018. A global slowdown of tropical-cyclone translation speed. *Nature* 558 (7708):104–107. doi: 10.1038/s41586-018-0158-3.

Kruk, M. C., E. J. Gibney, D. H. Levinson, and M. Squires. 2010. A climatology of inland winds from tropical cyclones for the eastern United States. *Journal of Applied Meteorology and Climatology* 49 (7):1538–47. doi: 10.1175/2010JAMC2389.1.

Landsea, C. W. 2007. Counting Atlantic tropical cyclones back to 1900. *EOS: Transactions of the American Geophysical Union* 88 (18):197–202. doi: 10.1029/2007EO180001.

Landsea, C. W., and J. L. Franklin. 2013. Atlantic hurricane database uncertainty and presentation of a new database format. *Monthly Weather Review* 141 (10):3576–92. doi: 10.1175/MWR-D-12-00254.1.

Landsea, C. W., R. A. Pielke, A. M. Mestas-Nunez, and J. A. Knaff. 1999. Atlantic basin hurricanes: Indices of climatic changes. *Climatic Change* 42 (1):89–129. doi: 10.1023/A:1005416332322.

Lane, P., J. P. Donnelly, J. D. Woodruff, and A. D. Hawkes. 2011. A decadally-resolved paleohurricane record archived in the late Holocene sediments of a Florida sinkhole. *Marine Geology* 287 (1–4):14–30. doi: 10.1016/j.margeo.2011.07.001.

Li, L., and P. Chakraborty. 2020. Slower decay of landfalling hurricanes in a warming world. *Nature* 587 (7833):230–34. doi: 10.1038/s41586-020-2867-7.

Lin, N., P. Lane, K. A. Emanuel, R. M. Sullivan, and J. P. Donnelly. 2014. Heightened hurricane surge risk in northwest Florida revealed from climatological-hydrodynamic modeling and paleorecord reconstruction. *Journal of Geophysical Research: Atmospheres* 119 (14):8606–23. doi: 10.1002/2014JD021584.

Liu, K. B., and M. L. Fearn. 1993. Lake-sediment record of late Holocene hurricane activities from coastal Alabama. *Geology* 21 (9):793–96. doi: 10.1130/0091-7613(1993)021<0793:LSROLH>2.3.CO;2.

Liu, K. B., and M. L. Fearn. 2000. Holocene history of catastrophic hurricane landfalls along the Gulf of Mexico coast reconstructed from coastal lake and marsh sediments. In *Current stresses and potential vulnerabilities: Implications of global change for the Gulf Coast region of the United States*,Vol. 223, ed. H. N. Zhu and K. K. Abdollahi, 39–47. Baton Rouge, LA: Franklin Press.

Malmstadt, J. C., J. B. Elsner, and T. H. Jagger. 2010. Risk of strong hurricane winds to Florida cities. *Journal of Applied Meteorology and Climatology* 49 (10):2121–32. doi: 10.1175/2010JAMC2420.1.

Malmstadt, J., K. Scheitlin, and J. Elsner. 2009. Florida hurricanes and damage costs. *Southeastern Geographer* 49 (2):108–31.

Misra, V., S. DiNapoli, and M. Powell. 2013. The track integrated kinetic energy of Atlantic tropical cyclones. *Monthly Weather Review* 141 (7):2383–89. doi: 10.1175/MWR-D-12-00349.1.

Muller, J., J. Collins, S. Gibson, and L. Paxton. 2017. Recent advances in the emerging field of paleotempestology. In *Hurricanes and climate change*, Vol. 3, ed. J. Collins and K. Walsh, 1–33. Springer.

Muller, J., C. Ercolani, J. Collins, and S. Ellis. 2022. Multi-proxy characterization of storm deposits in Sanibel Island, Florida: A modern analog for paleotempestology. *Geomorphology* 402:108148. doi: 10.1016/j.geomorph.2022.108148.

Muller, R. A., and G. W. Stone. 2001. A climatology of tropical storm and hurricane strikes to enhance vulnerability prediction for the southeast US coast. *Journal of Coastal Research* 17 (4):949–56.

Murnane, R. J., and J. B. Elsner. 2012. Maximum wind speeds and US hurricane losses. *Geophysical Research Letters* 39 (16): L16707. doi: 10.1029/2012GL052740.

National Oceanic and Atmospheric Administration (NOAA). 2012. The Saffir–Simpson hurricane wind scale. National Hurricane Center. Accessed April 27, 2022. https://www.nhc.noaa.gov/aboutsshws.php.

National Oceanic and Atmospheric Administration (NOAA). 2022. U.S. billion-dollar weather and climate disasters. Accessed April 27, 2022. https://www.ncdc.noaa.gov/billions/, doi: 10.25921/stkw-7w73.

Parisi, F., and R. Lund. 2008. Return periods of continental US hurricanes. *Journal of Climate* 21 (2):403–10. doi: 10.1175/2007JCLI1772.1.

Pasch, R. J., D. P. Brown, and E. S. Blake. 2004. NHC tropical cyclone report: Hurricane Charley. National Hurricane Center. Accessed July 3, 2022. https://www.nhc.noaa.gov/data/tcr/AL032004_Charley.pdf.

Pasch, R. J., A. S. Latto, and J. P. Cangialosi. 2019. NHC tropical cyclone report: Tropical Storm Emily. National Hurricane Center. Accessed September 25, 2022. https://www.nhc.noaa.gov/data/tcr/AL062017_Emily.pdf.

Pielke, R. A., Jr., and R. A. Pielke, Sr., eds. 1997. *Hurricanes: Their nature and impacts on society*. West Sussex, UK: Wiley.

Powell, M. D., and T. A. Reinhold. 2007. Tropical cyclone destructive potential by integrated kinetic energy. *Bulletin of the American Meteorological Society* 88 (4):513–26. doi: 10.1175/BAMS-88-4-513.

Truchelut, R. E., R. E. Hart, and B. Luthman. 2013. Global identification of previously undetected pre-satellite-era tropical cyclone candidates in NOAA/CIRES twentieth-century reanalysis data. *Journal of Applied Meteorology and Climatology* 52 (10):2243–59. doi: 10.1175/JAMC-D-12-0276.1.

Truchelut, R. E., and E. M. Staehling. 2017. An energetic perspective on United States tropical cyclone landfall droughts. *Geophysical Research Letters* 44 (23):12013–19. doi: 10.1002/2017GL076071.

U.S. Census Bureau. 2021. 2021 national and state population estimates and components of change. Accessed June 24, 2022. https://www.census.gov/newsroom/press-releases/2021/2021-population-estimates.html.

van Hengstum, P. J., J. P. Donnelly, M. R. Toomey, N. A. Albury, P. Lane, and B. Kakuk. 2014. Heightened hurricane activity on the Little Bahama Bank from 1350 to 1650 AD. *Continental Shelf Research* 86:103–15. doi: 10.1016/j.csr.2013.04.032.

Vecchi, G. A., C. Landsea, W. Zhang, G. Villarini, and T. Knutson. 2021. Changes in Atlantic major hurricane frequency since the late-19th century. *Nature Communications* 12 (1):1–9. doi: 10.1038/s41467-021-24268-5.

Villarini, G., and G. A. Vecchi. 2012. North Atlantic power dissipation index (PDI) and accumulated cyclone energy (ACE): Statistical modeling and sensitivity to sea surface temperature changes. *Journal of Climate* 25 (2):625–37. doi: 10.1175/JCLI-D-11-00146.1.

Williams, H., and E. Denlinger. 2013. Contribution of Hurricane Ike storm surge sedimentation to long-term aggradation of southeastern Texas coastal marshes. *Journal of Coastal Research* 65:838–43. doi: 10.2112/SI65-142.1.

Zhai, A. R., and J. H. Jiang. 2014. Dependence of US hurricane economic loss on maximum wind speed and storm size. *Environmental Research Letters* 9 (6):064019. doi: 10.1088/1748-9326/9/6/064019.

Zhou, Y., C. Matyas, H. Li, and J. Tang. 2018. Conditions associated with rain field size for tropical cyclones landfalling over the Eastern United States. *Atmospheric Research* 214:375–85. doi: 10.1016/j.atmosres.2018.08.019.

Zhu, Y.-J., and J. M. Collins. 2021. Recent rebounding of the post-landfall hurricane wind decay period over the continental United States. *Geophysical Research Letters* 48 (6):e2020GL092072. doi: 10.1029/2020GL092072.

Zhu, Y. J., J. M. Collins, and P. J. Klotzbach. 2021a. Nearshore hurricane intensity change and post-landfall dissipation along the United States Gulf and East Coasts. *Geophysical Research Letters* 48 (17):2021GL094680. doi: 10.1029/2021GL094680.

Zhu, Y.-J., J. M. Collins, and P. J. Klotzbach. 2021b. Spatial variations of North Atlantic landfalling tropical cyclone wind speed decay over the continental United States. *Journal of Applied Meteorology and Climatology* 60 (6):749–62. doi: 10.1175/JAMC-D-20-0199.1.

YI-JIE ZHU is a Postdoctoral Fellow at the Cooperative Institution for Research in the Atmosphere, Colorado State University, Fort Collins, CO 80521. E-mail: yijie.zhu@colostate.edu. He conducted this study while he was a PhD candidate at the University of South Florida. He will be joining Florida Atlantic University as an Assistant Professor starting in Fall 2023. His research interests include tropical cyclone postlandfall impact from both climatological and geographical aspects.

JENNIFER COLLINS is a Professor in the School of Geosciences at the University of South Florida, Tampa, FL 33620. E-mail: collinsjm@usf.edu. Her research interests include physical and social aspects of hurricanes including understanding active and inactive hurricane seasons and hurricane evacuation decision-making.

JOANNE MULLER is a Professor in the Department of Marine and Earth Sciences in the Water School at Florida Gulf Coast University, Fort Myers, FL 33965. E-mail: jmuller@fgcu.edu. Her current research interests center on past climate change in tropical and subtropical latitudes with a special focus on Florida hurricane reconstructions.

PHILIP KLOTZBACH is a Senior Research Scientist in the Department of Atmospheric Science at Colorado State University, Fort Collins, CO 80523. E-mail: philk@atmos.colostate.edu. His research interests include subseasonal and seasonal forecasting of hurricane activity and the impacts of climate change on hurricanes.